United States
Environmental Protection
Agency

Predicting Attenuation of Viruses During Percolation in Soils

1. Probabilistic Model

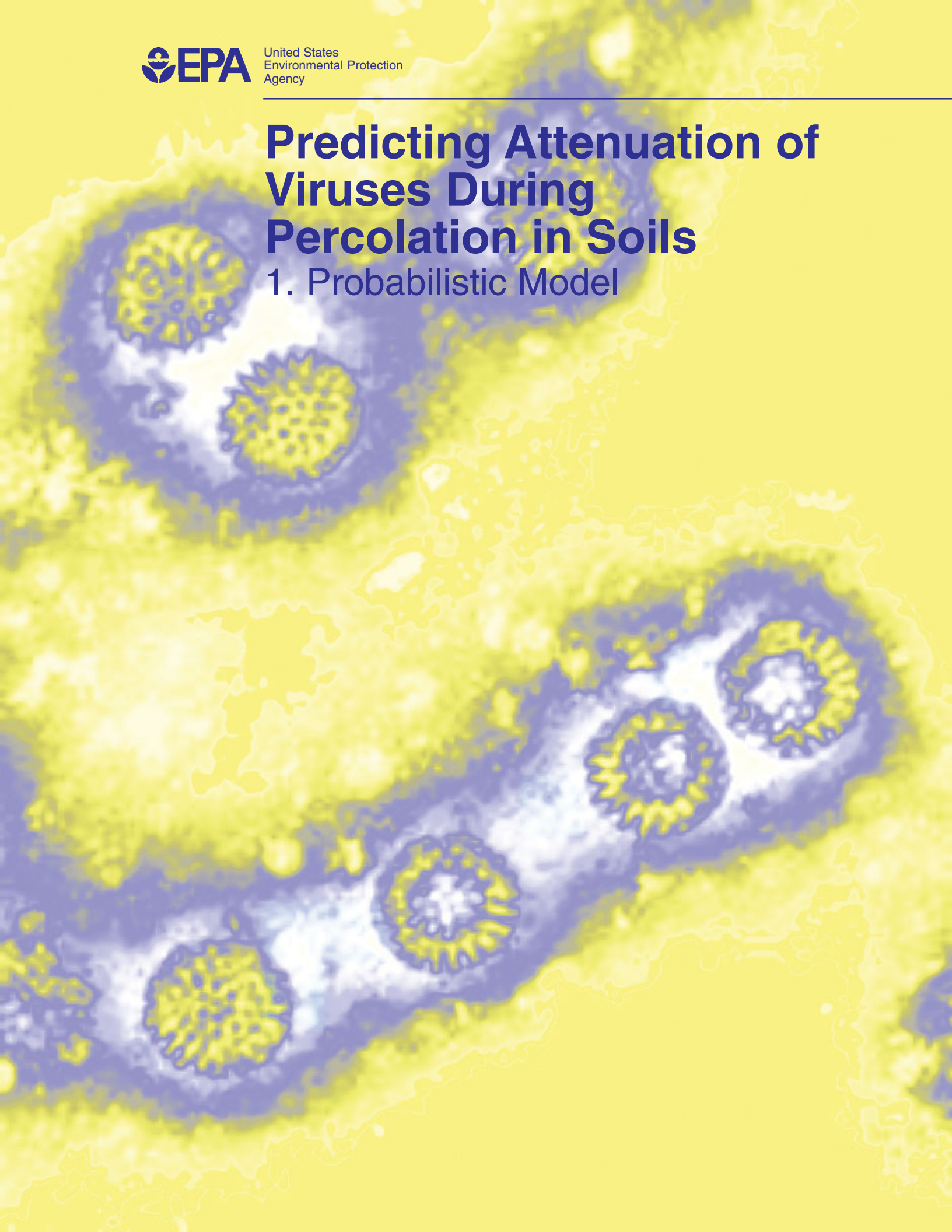

EPA/600/R-02/051a
August 2002

Predicting Attenuation of Viruses During Percolation in Soils: 1. Probabilistic Model.

Barton R. Faulkner
U.S. EPA Office of Research and Development
National Risk Management Research Laboratory
Subsurface Protection and Remediation Division
Ada, Oklahoma 74820

William G. Lyon
ManTech Environmental Research Services Corp.
Ada, Oklahoma 78420

Faruque A. Khan
U.S. EPA Headquarters
Washington, District of Columbia 20460

Sandip Chattopadhyay
Battelle Memorial Institute
Environmental Restoration Department
Columbus, Ohio 43230

Contract Number 68-C-98-138

Project Officer
Georgia A. Sampson

National Risk Management Research Laboratory
Office of Research and Development
U.S. Environmental Protection Agency
Cincinnati, OH 45268

Notice

The U.S. Environmental Protection Agency through its Office of Research and Development funded and managed the research described here through in-house efforts and under Contract 68-C-98-138 to ManTech Environmental Research Services Corporation. It has been subjected to the Agency's peer and administrative review and has been approved for publication as an EPA document. Use of trade names or commercial products does not constitute endorsement or recommendation for use.

All research projects making conclusions or recommendations based on environmental data and funded by the U.S. Environmental Protection Agency are required to participate in the Agency Quality Assurance Program. This project was conducted under an approved Quality Assurance Project Plan. The procedures specified in this plan were used without exception. Information on the plan and documentation of the quality assurance activities and results are available from the Principal Investigator.

Virulo and the user's guide have been subjected to the Agency's peer and administrative review and have been approved for publication as an EPA document. *Virulo* is made available on an as-is basis without guarantee or warranty of any kind, express or implied. Neither the United States Government (U.S. EPA), ManTech Environmental Research Services Corporation, Battelle Memorial Institute, Washington State Department of Ecology, nor any of the authors or reviewers accept any liability resulting from the use of *Virulo*, and interpretation of the predictions of the model are the sole responsibility of the user.

Foreword

The U.S. Environmental Protection Agency is charged by Congress with protecting the Nation's land, air, and water resources. Under a mandate of national environmental laws, the Agency strives to formulate and implement actions leading to a compatible balance between human activities and the ability of natural systems to support and nurture life. To meet this mandate, EPA's research program is providing data and technical support for solving environmental problems today and building a science knowledge base necessary to manage our ecological resources wisely, understand how pollutants affect our health, and prevent or reduce environmental risks in the future.

The National Risk Management Research Laboratory (NRMRL) is the Agency's center for investigation of technological and management approaches for preventing and reducing risks from pollution that threatens human health and the environment. The focus of the Laboratory's research program is on methods and their cost-effectiveness for prevention and control of pollution to air, land, water, and subsurface resources; protection of water quality in public water systems; remediation of contaminated sites, sediments and ground water; prevention and control of indoor air pollution; and restoration of ecosystems. NRMRL collaborates with both public and private sector partners to foster technologies that reduce the cost of compliance and to anticipate emerging problems. NRMRL's research provides solutions to environmental problems by: developing and promoting technologies that protect and improve the environment; advancing scientific and engineering information to support regulatory and policy decisions; and providing the technical support and information transfer to ensure implementation of environmental regulations and strategies at the national, state, and community levels.

EPA's Office of Water is currently promulgating a Ground Water Rule to ensure water supplies are safe from contamination by viruses. States may be required to conduct *hydrogeologic sensitivity assessments* to predict whether a particular aquifer is vulnerable to pathogens. This work presents the conceptual and theoretical development of a predictive screening model for virus attenuation above aquifers. It is hoped this model will be a useful tool for State regulators, utilities, and development planners.

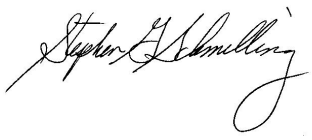

Stephen G. Schmelling, Acting Director
Subsurface Protection and Remediation Division
National Risk Management Research Laboratory

Abstract

We present a probabilistic model for predicting virus attenuation. Monte Carlo methods are used to generate ensemble simulations of virus attenuation due to physical, biological, and chemical factors. The model generates a probability of failure to achieve a chosen degree of attenuation. We tabulated data from related studies to develop probability density functions for input parameters, and utilized a database of soil hydraulic parameters based on the 12 USDA soil categories. Regulators can use the model based on limited information such as boring logs, climate data, and soil survey reports for a particular site of interest. The model may be most useful as a tool to aid in siting new septic systems.

Sensitivity analysis indicated the most important main effects on probability of failure to achieve 4-log (99.99%) attenuation in our model were mean logarithm of saturated hydraulic conductivity (+0.105) and the rate of microscopic mass transfer of suspended viruses to the air-water interface (−0.099), where they are permanently adsorbed and removed from suspension in the model. Using the model, we predicted the probability of failure of a 1-meter thick proposed hydrogeologic barrier to achieve 4-log attenuation. Assuming a soil water content of 0.3, with the currently available data and the associated uncertainty, we predicted the following probabilities of failure: sand ($p = 22/5697$), silt loam ($p = 6/2000000$), and clay ($p = 0/9000000$).

The model is extensible in the sense that probability density functions of parameters can be modified as future studies refine the uncertainty, and the lightweight object-oriented design of the computer model (implemented in Java™) will facilitate reuse with modified classes, and implementation in a geographic information system.

Contents

List of Figures

List of Tables

Acknowledgments

The authors would like to thank Mohamed Hantush, U.S. EPA, for his invaluable suggestion to use the final value theorem modeling approach, and many other helpful suggestions. We would also like to thank John Wilson of the U.S. EPA for providing compiled data, Kathy Tynsky (Computer Sciences Corp.) for designing the graphics on the cover, and Joan Elliott (U.S. EPA) and Martha Williams (Computer Sciences Corp.), for their advice in typesetting this document.

1 Introduction

Impending regulations in U.S. EPA's forthcoming Ground Water Rule (EPA, 2000) will require public water systems (PWS) to more closely monitor their ground-water systems for contamination by pathogenic viruses. The Rule clarifies the conditions that define risk to PWS from viruses. Regulators can use the new definitions for siting new septic systems. If it can be shown that the risk is low due to the presence of a hydrogeologic barrier, a proposed site may be acceptable. The Rule defines a hydrogeologic barrier as a subsurface region through which viruses must pass from a source in order to reach PWS wells that provides at least a yet undetermined, but specific degree of attenuation of active pathogenic viruses. The draft rule indicates attenuation factors are "physical, biological, and chemical" acting "singularly or in combination."

In instances where the ground-water system in question is connected to potential virus sources by karst, fractured rock, gravel, or a soil exhibiting preferential flow, the system will be classified as high risk. In other cases the assessment process will benefit from prediction by mathematical modeling. Therefore, regulators and utility operators may benefit from simple, probabilistic quantitative models as tools in the context of responding to the Ground Water Rule (GWR). This document presents the development of a proposed model to evaluate attenuation as viruses are carried with percolating water in an unsaturated, naturally existing soil layer. The model itself is a computer application. At the time of this writing, a user's guide for this model is imminent in a companion document. Here we describe the conceptual and mathematical development of the model, and highlight areas of much needed research.

2 Abridged Literature Review

Although several papers describing the modeling of virus transport in ground water have recently been published, there is not yet a concensus on which factors have the greatest impact on eliminating active viruses as they pass through natural porous media. Keswick and Gerba (1980) presented an early review of factors affecting viruses in ground water. More recently, Schijven and Hassanizadeh (2000) wrote a valuable review that is fairly comprehensive, and Breidenbach et al. (in review) have produced an environmental handbook and extensive bibliography on the subject. We refer the reader to these works for a description of the available data from field and laboratory studies.

Current modeling approaches have been criticized. Yates (1995) demonstrated, by using a numerical dynamic model to predict virus survival, that field data do not agree well with model predictions. In particular, their model-predicted attenuation was dramatically greater than actual. Yates and Jury (1995) have emphasized the sensitivity of a numerical dynamic model to input parameters.

Modeling approaches themselves have varied greatly depending on the scale of the study and the specific interests of the investigators. Some treat virus transport as

a Fickian process, coupled with advection of ground water; others have incorporated filtration theory, treating virus transport as a colloid filtration process.

Field studies in which viruses were released into the subsurface have documented early arrival times, with arrivals at monitoring wells sometimes preceding those of dissolved tracers. Viruses are more likely to be attenuated during percolation in the unsaturated zone than during transport through the same distance in the saturated zone (Lance and Gerba, 1984). Studies with unsaturated soils have shown that hydrophobic colloids are adsorbed at the air-water interface in greater proportion than the mineral-water interface (Wan and Wilson, 1994), and this is apparently also the case with viruses (Thompson et al., 1998; Thompson and Yates, 1999). Chu et al. (2001) have shown that when sand column experiments were conducted with reactive solids removed (metals and metal oxides) the effect of the air-water interface was most pronounced, and suggested reactions at the solid-water interface may be dominant when reactive solids are present. Sim and Chrysikopoulos (2000) developed a governing constitutive equation for unsaturated-zone virus transport that considers partitioning of viruses to the air-water interface. More recently, Chu et al. (2001) expanded this model, more closely considering interfacial reactions using as yet untabulated parameters.

3 Mathematical Description

3.1 Differential Equations

Sim and Chrysikopoulos (2000) developed the following governing equation which can describe the transport of viruses in a porous medium as depicted in Figure 1:

$$\frac{\partial[\theta_m C]}{\partial t} + \rho\frac{\partial C^*}{\partial t} + \frac{\partial[\theta_m C^\diamond]}{\partial t} = D_z\theta_m\frac{\partial^2 C}{\partial z^2} - \frac{\partial[qC]}{\partial z} - \lambda\theta_m C - \lambda^*\rho C^* - \lambda^\diamond\theta_m C^\diamond \quad (1)$$

where $C = C(t,z)$ (ML^{-3}) is the concentration of viruses in the mobile solution phase, t is time, z (L) is the downward distance from the top of the proposed hydrogeologic barrier, $C^*(t,z)$ (MM^{-1}) is the adsorbed virus concentration at the liquid-solid interface, $C^\diamond(t,z)$ (ML^{-3}) is the adsorbed virus concentration at the liquid-air interface, q (LT^{-1}) is the specific discharge, θ_m (L^3L^{-3}) is the moisture content, λ (T^{-1}) is the inactivation rate coefficient for the viruses in the bulk solution, λ^* (T^{-1}), the inactivation rate for the viruses that are sorbed at the liquid-solid interface, and $\lambda^\diamond$ (T^{-1}), the inactivation rate for the viruses sorbed at the liquid-air interface, ρ (ML^{-3}) is the soil bulk density, and $D_z = \alpha_z q/\theta_m + \mathcal{D}_e$ (L^2T^{-1}) is the hydrodynamic dispersion coefficient, α_z (L) is the vertical dispersivity, $\mathcal{D}_e = \mathcal{D}/\tau$ (L^2T^{-1}), where $\mathcal{D}$ (L^2T^{-1}) is the virus diffusivity in water, and τ $(LL^{-1}$, greater than 1) is the tortuosity.

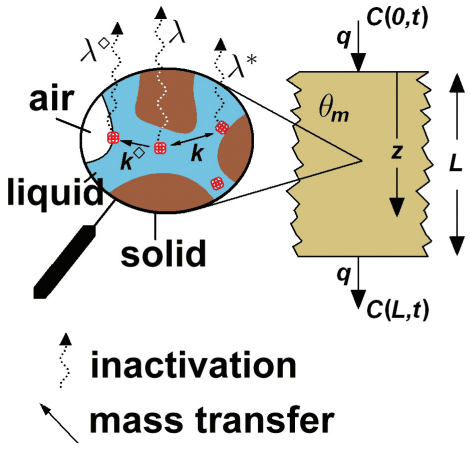

Figure 1: **Processes Considered in the Model.**

We assumed the following:

- Steady-state flow
- Gravity drainage only
- The soil is homogeneous in terms of
  - hydraulic properties
  - virus properties
  - geochemistry
- The soil does not induce preferential flow

Sorption and inactivation of viruses at the various interfaces is described by Sim and Chrysikopoulos (2000) by

$$\rho \frac{\partial C^*}{\partial t} = k\theta_m \left(C - \frac{C^*}{K_d} \right) - \lambda^* \rho C^* \tag{2}$$

where $k = \kappa a_T$, $a_T = 3(1-\theta_s)/r_p$ is the liquid-solid interfacial area in units of (L^2L^{-3}). The symbol k (T^{-1}) is the microscopic mass transfer rate and κ (LT^{-1}) is called the mass transfer coefficient. In Eq. 2, K_d (L^3M^{-1}) is the equilibrium partitioning coefficient, r_p (L) is the average radius of soil particles, and θ_s (L^3L^{-3}) is the saturated water content. Analogously they derived the change in concentration of viable viruses at the air-water interface,

$$\theta_m \frac{\partial C^\diamond}{\partial t} = k^\diamond \theta_m C - \lambda^\diamond \theta_m C^\diamond \tag{3}$$

where $k^{\diamond}$ (T^{-1}) is the liquid to liquid-air interface mass transfer rate. The mass transfer rate for the liquid to liquid-air interface is described by

$$k^{\diamond} = \kappa^{\diamond} a_T^{\diamond} \tag{4}$$

where $\kappa^{\diamond}$ $(L^2 L^{-3})$ is the mass transfer coefficient and $a_T^{\diamond}$ is the estimated area of the air-liquid interface as a function of the moisture content. Thompson et al. (1998) and Thompson and Yates (1999) have demonstrated dependence of viral inactivation rates on their sorption state. A method for estimating $a_T^{\diamond}$ is discussed below in the section on Mass Transfer and Inactivation Rates.

The Buckingham-Darcy flow equation for the downward water flux in the unsaturated zone is (Jury et al., 1991, p. 88):

$$q = K(h) \left(\frac{\partial [h + z]}{\partial z} \right) \tag{5}$$

where h (L) is the capillary pressure head and z is positive downward.

3.2 Proposed Solution for the Differential Equations

Using the above governing equations, we would like to determine whether a proposed hydrogeologic barrier is likely to produce a specified degree (ε-log) of attenuation. To solve the equations we will formulate an attenuation function $f(t, z)$ for percolating viruses, and focus our interest on the *cumulative* attenuation, the total mass leached (M) at depth z from the bottom of the barrier $(z = L)$. Considering a unit area portion of the barrier bottom, the leached mass is (Hantush et al., 2000):

$$M(t, z = L) = \int_0^t f(\omega, z = L) d\omega \Bigg|_{t \to \infty} \tag{6}$$

We will apply the *final value theorem* of operational mathematics. This theorem states that given the Laplace transform $\tilde{M}(s, z)$ of the cumulative attenuation, the following identity holds (Hantush et al., 2000):

$$\lim_{t \to \infty} M(z) = \lim_{s \to 0} s\tilde{M}(s, z) \tag{7}$$

In other words, we can determine the final value of the cumulative attenuation function M by simply taking its Laplace transform, $\tilde{M}$, and evaluating it as the Laplace domain variable $s \to 0$. Although this conceptualization is traditionally used in the design of chemical reactors, Hantush et al. (2000) have shown the conditions under which it may be valid for transport in natural environmental systems. They discuss the differences between a complete mixing model and the more realistic advective-dispersive model, applied to the final value of attenuation.

Figure 1 is our conception of a proposed natural hydrogeologic barrier. The output consists of remaining viable viruses plus the amount destroyed due to the attenuation factors of suspension and sorption coupled with virus-specific degradation rates.

The initial and boundary conditions are:

$$C(0,z) = C^{*}(0,z) = C^{\diamond}(0,z) = 0 \tag{8}$$

$$\frac{\partial C(t,\infty)}{\partial z} = 0 \tag{9}$$

Mass continuity through the upper boundary requires the additional boundary condition which states the input equals the supplying concentration, subject to the advection and dispersion constraints of the porous medium:

$$f(t,0) = qC_{max}e^{-\beta t} = -D_z\theta_m \frac{\partial C}{\partial z}\bigg|_{z=0} + qC\bigg|_{z=0} \tag{10}$$

Since it is assumed that the flow is due to gravity only($\partial h/\partial z = 0$), then the total head gradient is unity $(\partial z/\partial z)$ and $q = K(\theta_m)$. To obtain $K(\theta_m)$, van Genuchten (1980) obtained the following:

$$K(\theta_m) = K_s\left(\frac{\theta_m - \theta_r}{\theta_s - \theta_r}\right)^{\frac{1}{2}}\left[1 - \left[1 - \left(\frac{\theta_m - \theta_r}{\theta_s - \theta_r}\right)^{\frac{n}{n-1}}\right]^{1-\frac{1}{n}}\right]^2 \tag{11}$$

where K_s is the saturated hydraulic conductivity, θ_r is the residual water content (L^3L^{-3}), θ_s is the saturated water content (L^3L^{-3}), and n is a well-tabulated empirical curve fitting parameter (Table 1).

We consider the case where the supplying concentration results from percolation of water containing viruses lasting for a period of time that is small compared to the residence time in a proposed barrier. Such a situation would result if a septic tank temporarily overflowed and was then pumped or otherwise corrected, thereby stopping the virus source. Arrival of viruses at the input may be approximated as a relatively sharp concentration front followed by exponentially decreasing concentration of viruses, such that the concentration of viruses immediately above the upper boundary region of the barrier is $C_{max}\exp[-\beta t]$. Now we can write the attenuation function:

$$f(t,z) = -D_z\theta_m\frac{\partial C}{\partial z} + qC \tag{12}$$

Having made the above assumptions, and assuming dispersion and bulk density of the soil are constant throughout the proposed barrier, taking the Laplace transform of Eq. 1, and applying the intial conditions (Eq. 8) yields

Table 1: **Hydraulic Properties of Sand, Silt, and Clay**

Soil*	Parameter	N	Mean	Standard Deviation	Units
sand	θ_r	308	0.050	0.003	L^3L^{-3}
	θ_s	308	0.367	0.032	L^3L^{-3}
	$\log_{10}K_s$	99¶	-0.691	0.218	$\log(m\ hr^{-1})$
	$\log_{10}\alpha$	308	0.5306	0.034	$\log(m^{-1})$
	$\log_{10}n$	308	0.482	0.077	$\log(dimensionless)$
	ρ	168¶	1.58×10^6	1.42×10^5	$g\ m^{-3}$
	r_p	0§	4.71×10^{-4}	1.60×10^{-5}	m
	α_z	1†	5.59×10^{-3}	0.00	m
	T	1944⋆	11.7	7.38	$^\circ\ Celsius$
silt loam	θ_r	330	0.063	0.013	L^3L^{-3}
	θ_s	330	0.406	0.050	L^3L^{-3}
	$\log_{10}K_s$	75¶	-2.160	-0.384	$\log(m\ hr^{-1})$
	$\log_{10}\alpha$	330	-0.207	0.075	$\log(m^{-1})$
	$\log_{10}n$	330	0.206	0.016	$\log(dimensionless)$
	ρ	133¶	1.43×10^6	1.48×10^5	$g\ m^{-3}$
	r_p	0§	1.18×10^{-4}	5.50×10^{-5}	m
	α_z	1‡	8.75×10^{-5}	0.00	m
	T	1944⋆	11.7	7.38	$^\circ\ Celsius$
clay	θ_r	84	0.101	0.011	L^3L^{-3}
	θ_s	84	0.515	0.085	L^3L^{-3}
	$\log_{10}K_s$	22¶	-2.085	0.0475	$\log(m\ hr^{-1})$
	$\log_{10}\alpha$	84	0.276	0.129	$\log(m^{-1})$
	$\log_{10}n$	84	0.114	0.015	$\log(dimensionless)$
	ρ	38¶	1.29×10^6	1.68×10^5	$g\ m^{-3}$
	r_p	0§	9.95×10^{-5}	6.15×10^{-5}	m
	α_z	1‡	8.75×10^{-5}	0.00	m
	T	1944⋆	11.7	7.38	$^\circ\ Celsius$

* Generated with the *Rosetta* program (Schaap et al. 1999). unless otherwise noted.
† Field lysimeter study by Poletika et al. (1995).
‡ Kaczmarek et al. (1997).
⋆ Data from *Remote Soil Temperature Network* [1].
¶ From the *UNSODA* database (Leij et al. 1996).
§ Generated with random deviates in soil textural triangle queried by *USDA* category.

$$\theta_m s\tilde{C} + \rho s\tilde{C}^* + \theta_m s\tilde{C}^\diamond = D_z\theta_m\frac{d^2\tilde{C}}{dz^2} - q\frac{d\tilde{C}}{dz} - \lambda\theta_m\tilde{C} - \lambda^*\rho\tilde{C}^* - \lambda^\diamond\theta_m\tilde{C}^\diamond \quad (13)$$

Likewise, the Laplace transform of Eq. 2 is

$$\rho s\tilde{C}^* = k\theta_m\left(\tilde{C} - \frac{\tilde{C}^*}{K_d}\right) - \lambda^*\rho\tilde{C}^* \quad (14)$$

Likewise, the Laplace transform of Eq. 3 is

$$\theta_m s\tilde{C}^\diamond = k^\diamond\theta_m\tilde{C} - \lambda^\diamond\theta_m\tilde{C}^\diamond \quad (15)$$

Noting the boundary conditions given by Eq. 8, and solving for $\tilde{C}^*$ in Eq. 14, we obtain

$$\tilde{C}^*(s,z) = \frac{1}{\frac{\rho s}{k\theta_m} + \frac{1}{K_d} + \frac{\lambda^*\rho}{k\theta_m}}\tilde{C}(s,z) \quad (16)$$

We can solve for $\tilde{C}^\diamond$ in Eq. 15 to obtain

$$\tilde{C}^\diamond(s,z) = \frac{k^\diamond}{s+\lambda^\diamond}\tilde{C}(s,z) \quad (17)$$

Now we insert the substitutions into Eq. 13, which yields the following ordinary differential equation, in terms of $\tilde{C}$:

$$D_z\frac{d^2\tilde{C}}{dz^2} - \overline{V}\frac{d\tilde{C}}{dz} - \dot{\gamma}\tilde{C} = 0 \quad (18)$$

where

$$\dot{\gamma} = \lambda + \frac{\lambda^*\rho}{\left(\frac{\rho s}{k} + \frac{\theta_m}{K_d} + \frac{\lambda^*\rho}{k}\right)} + \frac{\lambda^\diamond k^\diamond}{s+\lambda^\diamond} + s + \frac{\rho s}{\left(\frac{\rho s}{k} + \frac{\theta_m}{K_d} + \frac{\lambda^*\rho}{k}\right)} + \frac{sk^\diamond}{s+\lambda^\diamond} \quad (19)$$

To solve Eq. 18 we consider the homogeneous equation which has the characteristic polynomial $D_z\Gamma^2 - \overline{V}\Gamma - \dot{\gamma}$. The general solution is $\tilde{C}(s,z) = \varphi_1 \exp[\Gamma_1(s)z] + \varphi_2 \exp[\Gamma_2(s)z]$, where, by the quadratic formula

$$\Gamma_1(\dot{\gamma}) = \frac{\overline{V} + \sqrt{\overline{V}^2 + 4D_z\dot{\gamma}}}{2D_z}, \qquad \Gamma_2(\dot{\gamma}) = \frac{\overline{V} - \sqrt{\overline{V}^2 + 4D_z\dot{\gamma}}}{2D_z} \tag{20}$$

The Laplace transform of Eq. 9 is $d\tilde{C}(s,\infty)/dz$, which implies $\varphi_1 = 0$ for a physically reasonable solution, thus $\tilde{C}(s,z) = \varphi_2 \exp[\Gamma_2(s)z]$.

The Laplace transform of Eq. 12 is

$$\tilde{f}(s,z) = -D_z\theta_m \frac{d\tilde{C}}{dz} + q\tilde{C} \tag{21}$$

Substituting for $\tilde{C}$ and its derivative, we have:

$$\tilde{f}(s,z) = -D_z\theta_m\varphi_2 e^{\Gamma_2 z}\Gamma_2 + q\varphi_2 e^{\Gamma_2 z} \tag{22}$$

The Laplace transform of Eq. 10 is

$$\tilde{f}(s,0) = \frac{qC_{max}}{s+\beta} = -D_z\theta_m \frac{d\tilde{C}(s,z)}{dz}\bigg|_{z=0} + q\tilde{C}\bigg|_{z=0} \tag{23}$$

or

$$-D_z\theta_m\varphi_2\Gamma_2\left(\dot{\gamma}(s)\right) + q\varphi_2 = \frac{qC_{max}}{s+\beta} \tag{24}$$

Thus, we find the value of φ_2 is

$$\varphi_2 = \frac{qC_{max}}{(s+\beta)\left(q - D_z\theta_m\Gamma_2\left(\dot{\gamma}(s)\right)\right)} \tag{25}$$

From Eq. 22:

$$\tilde{f}(s,z) = \frac{qC_{max}(q - D_z\theta_m\Gamma_2)}{(s+\beta)(q - D_z\theta_m\Gamma_2)} e^{\Gamma_2(\dot{\gamma}(s))z} = \frac{qC_{max}e^{\Gamma_2(\dot{\gamma}(s))z}}{s+\beta} \tag{26}$$

From Eq. 19, we note

$$\gamma = \lim_{s\to 0}\dot{\gamma} = \lambda + \frac{\lambda\rho}{\frac{\theta_m}{K_d} + \frac{\lambda^*\rho}{k}} + k^{\diamond} \tag{27}$$

We now apply the final value theorem:

$$\lim_{t\to\infty} M(z=L) = \lim_{s\to 0} \tilde{M}(s,z) = \frac{qC_{max}e^{\Gamma_2(\gamma)z}}{\beta} \tag{28}$$

The attenuation factor A is

$$A = \frac{M(z=L)}{M(z=0)} \tag{29}$$

To find $M(z=0)$, we integrate the input flux in time:

$$M(z=0) = qC_{max}\int_0^t e^{-\beta\omega}d\omega \;\Big|_{t\to\infty} = \frac{qC_{max}}{\beta} \tag{30}$$

thus

$$A = e^{\Gamma_2(\gamma)L} \tag{31}$$

The average velocity of the percolating water is $\bar{V} = q/\theta_m$. Note the inactivation rate for the air-water interface drops out of the final expression. This is due to the fact mass transfer to the air-water interface is irreversible; therefore, the rate of decay is irrelevant after the virus moves to the air-water interface from the mobile phase. We also note β drops out, because in the limit $t \to \infty$ the exponentially decaying input pulse appears as an instantaneous input of mass. It thus does not behave differently from the Dirac-δ pulse which has been used to model pesticide application (e.g., Hantush et al., 2000). The input concentration C_{max} also drops out because we are only interested in the attenuation factor.

We can now define a hydrogeologic barrier as a layer physically separating the virus source and the ground-water supply under consideration which produces the attenuation factor:

$$A =< 10^{-\varepsilon}, \;\; \texttt{or} \;\; -\log_{10}A > \varepsilon \tag{32}$$

For example, the current draft GWR frequently refers to a target value of $\varepsilon = 4$, meaning "4-log attenuation," or 99.99% attenuation of active viruses.

4 Mass Transfer and Inactivation Rates of Viruses

As viruses are carried with percolating water, their rate of inactivation depends on many factors. Breidenbach et al. (2001) provided an overview and tabulation of measured inactivation rates. Factors include the geochemical characteristics of the

Table 2: **Parameters Used for Poliovirus**

Parameter*	N	Mean	Standard Deviation	Units
$\log_{10}\lambda$	12	0.605	0.608	$\log(hr^{-1})$
$\log_{10}\lambda^*$	0‡	0.304	0.608	$\log(hr^{-1})$
κ	1†	1.34×10^{-3}	1.80×10^{-3}	$m\ hr^{-1}$
$\kappa^\diamond$	1†	9.27×10^{-3}	1.80×10^{-3}	$m\ hr^{-1}$
r_v	0§	1.375×10^{-8}	1.25×10^{9}	
K_d (sand)	87	2.43×10^{-4}	5.66×10^{-4}	$m^3\ g^{-1}$
K_d (silt loam)	23	3.77×10^{-4}	7.16×10^{-4}	$m^3\ g^{-1}$
K_d (clay)	39	7.20×10^{-4}	9.74×10^{-4}	$m^3\ g^{-1}$

* Data complied by Breidenbach et al. (2001) unless otherwise noted.
† From Chu et al. (2001), see Appendix A for assumptions.
‡ Yates and Ouyang (1992) assumed $\lambda^* \approx \lambda/2$.
§ Mazzone (1998) p. 114.

soil and water, such as temperature, pH, organic matter, and presence of metals or other ions.

Most of the work related to natural hydrogeologic barriers has been conducted with bacteriophages (viruses to bacteria), due to the restrictive conditions required to obtain such data for human pathogenic viruses without posing a risk to researchers. The polio viruses are perhaps the most widely studied human pathogenic viruses in this context. Table 2 lists the relevant properties of the viruses, based on Breidenbach et al. (2001). The data cover a fairly wide range of geochemical conditions, hence the high standard deviations. Measured mass transfer rate data is largely lacking. Vilker and Burge (1980) did early work that included some measurements for poliovirus. More recently, Chu et al. (2001) measured mass transfer parameters with *MS-2* bacteriophage, which has comparable size and geometric properties, using an inverse modeling approach.

Due to the difficulty of obtaining good experimental control, and the corresponding sparsity of data, a popular semi-empirical correlation to estimate κ, due to Wilson and Geankoplis (1966), $\kappa = 1.09\bar{V}^{\frac{1}{3}}\left[\mathcal{D}/2r_p\theta_s\right]^{\frac{2}{3}}$ is often employed. This correlation can be used at low Reynolds numbers, however, comparison between this expression and measured values shows very poor correlation (Pearson's correlation coefficient, $\rho_{pn} = 0.039$, $N = 23$). The expression fails to account for major factors that affect mass transfer of viruses at the molecular level, such as pH-dependent electrostatic interactions between the protein surfaces and soil particles and/or the air-water interface. Indeed the correlation was not developed for this purpose. The work of Chu et al. (2000) highlighted the enormous effect of oxides on sand grains in their soil column experiments. Their work suggested the pH-dependent behavior of oxide coatings has a stronger effect on mass transfer than the air-water interface. Much additional work is needed to develop realistic correlations to estimate mass transfer of viruses. The experimental control needed to conduct such studies can be daunting. Most soil column studies must rely on plaque assay methods that suffer from virus aggregation effects and other sources of uncertainty.

As with κ, a correlation has not been established for $\kappa^{\diamond}$ though we may now rely on the results of Chu et al (2001). These are listed in Table 2.

Rose and Bruce (1949) derived equations to estimate the air-water interfacial area by $a_T^{\diamond} = (\rho_w g h \theta_m)/\sigma$. In this expression, σ (MLT^{-2}) is the surface tension of water, ρ_w is the density of water, g is the acceleration due to gravity. Employing the van Genuchten (1980) expression that relates θ_m to the capillary pressure head h, and expressing the *effective saturation* as $S_e = (\theta_m - \theta_r)/(\theta_s - \theta_r)$ we obtain the following:

$$a_T^{\diamond} = \frac{\rho_w g \theta_m}{\alpha \sigma} \left[\left[S_e^{-1} \right]^{\frac{1}{1-1/n}} - 1 \right]^{1/n} \tag{33}$$

The benefit of using this expression is that it utilizes the well-tabulated fitting parameters for which we have already developed multivariate distribution functions which we will discuss in the next section.

Virus diffusivity $\mathcal{D}$ (L^2T^{-1}) is governed by Brownian motion and is described by the Stokes-Einstein equation:

$$\mathcal{D} = \frac{k_b T}{6\pi\mu r_v} \tag{34}$$

in which k_b is Boltzman's constant (MLT^{-2}), T ($^{\circ}$ Celsius) is temperature, $\mu = \mu(T)$ is viscosity of water $(ML^{-1}T^{-1})$, and r_v is the equivalent radius of the virus.

5 Modeling under Uncertainty

The draft Ground Water Rule states a specified degree of attenuation must occur in order for a hydrogeologic medium to be considered a barrier. Using the mathematical model with as much information about the geochemistry and other factors that can help in making a decision on the appropriate parameters, we operate under the premise that it is possible to obtain a prediction of attenuation that is more useful than a qualitative expression of confidence that the barrier can or cannot attenuate a particular virus. It is essential to develop a probabilistic expression of the confidence that $\varepsilon -$ log attenuation will occur, encapsulating the possible sources of error in the model parameters.

Virus diffusivity, $\mathcal{D}$, is a physical parameter that can be calculated if the temperature, T, and corresponding viscosity of water are known. Unfortunately, the tortuosity, τ, is less easily measured, since it depends not only on the modal particle diameter, but also the pore geometry and connectedness of the pores. Tortuosity for unsaturated soils is often predicted with (Schaefer et al., 1995):

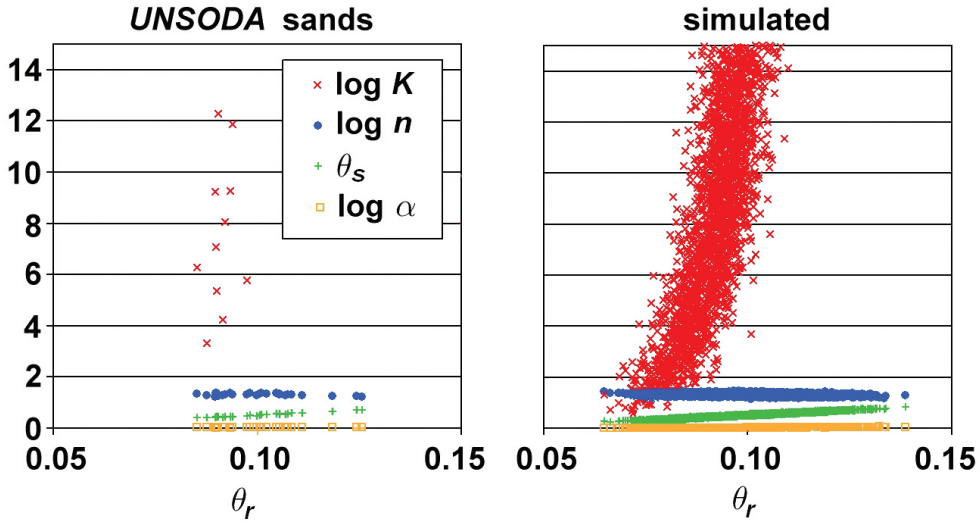

Figure 2: **Plot illustrating correlation of $\log_{10}K_s$, $\log_{10}n$, θ_s, and $\log_{10}\alpha$ with θ_r for sands in the UNSODA soils database and a corresponding multivariate normal ensemble simulation.**

$$\tau(\theta_m) = \begin{cases} \frac{\theta_s^2}{\theta_m^{11/5}} & \text{if } \theta_m \leq 0.2 \\ \\ \frac{\theta_s^2}{\theta_m^{7/3}} & \text{otherwise} \end{cases} \tag{35}$$

Although the data in Tables 1 and 2 list uncertainties that could introduce significant error into the predicted attenuation, we needn't rely on these variabilities as independent (orthogonal) sources of error. Many of the parameters, when measured in controlled experiments, are correlated. Thus we can consider their space of variability as conditionally multivariate normal and/or lognormal. The five parameters that display significant correlation (based on H_0: $\rho_{pn} = 0$, H_1: $\rho_{pn} \neq 0$) are shown in Figure 2.

We applied covariance- and histogram-honoring simulations using the Monte Carlo approach. Details of the Cholesky decomposition approach we used are described by other authors (e.g., see Kitanidis, 1997, Appendix C3). For all the other parameters, the Monte Carlo simulation used histograms from the parameters independently. The advantage of the Monte Carlo method is that it produces a histogram of attenuation factors as output and it allows us to assign a probability of failure to achieve $\varepsilon -$ log attenuation. Figure 2 shows the space of variability for the five (hydraulic) parameters which were significantly correlated. The simulated values were generated by conditional simulation of multivariate normal density functions parameterized by the variance-covariance matrices of the parameters, as determined with the *UNSODA* database (Leij et al., 1996). These are listed in Appendix B.

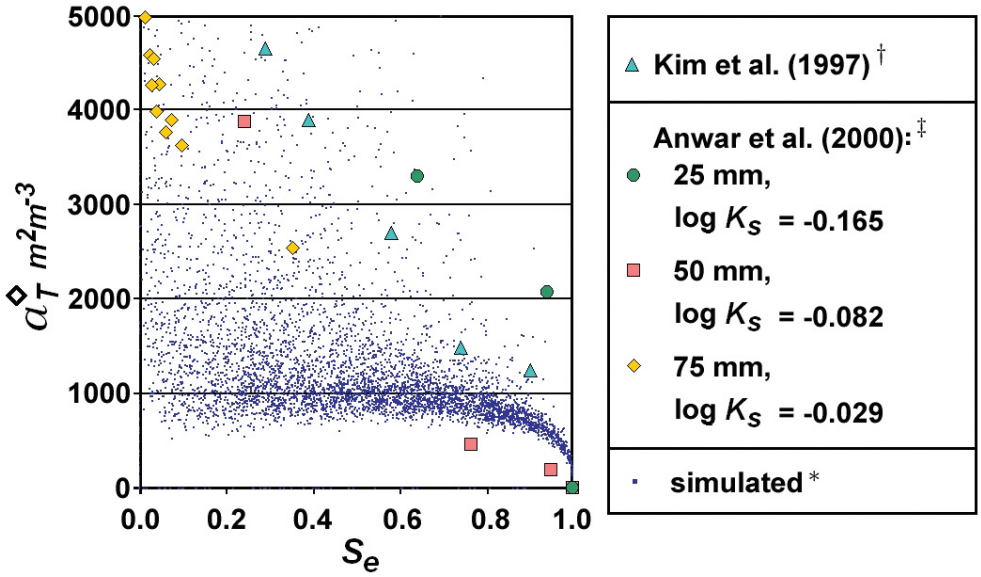

† Baked blasting sand.

‡ Glass micro-beads of 3 different mean diameters listed.

* Generated by setting mean $\theta_m = 0.16$, std. err. 0.2.

Figure 3: **Comparison of values of $a_T^\diamond$ used in model simulation for Rosetta sands with measured values.**

Recently, workers have measured air-water interfacial areas for partially saturated sand (Kim et al., 1997) and for variously-sized glass microbeads (Anwar et al., 2000). A comparison between these measurements and a conditional simulation is presented in Figure 3. The simulated values were obtained by using the multivariate probability density functions with the means for sand as obtained from the *Rosetta* program (Schaap et al., 1999).

Clearly, this simple model appears to underestimate $a_T^{\diamond}$ when S_e is less than about 0.6 (θ_m less than about 0.25). The measurements themselves may be subject to considerable error, and there is no data for finer soils and soils containing clays. At low water contents $a_T^{\diamond}$ will apparently be underestimated for sandy soils, thus the model should not be used to test barriers which are proposed solely on account of low water contents. Other means of evaluation should be used in those cases.

Figure 4 shows histograms of attenuation factors of polio 1 virus using the data in Tables 1 and 2, for 1 meter thick soils at water content equal to 0.30. The histograms were generated with Monte Carlo simulations with soil hydraulic data from the *UNSODA* soils database (Leij et al., 1996) for categorical sand and silt loam soils (Table 1). The soil values themselves were generated in previous studies using a bootstrap method (Schaap et al., 1999). The uncertainty associated with hydraulic parameters is relatively well understood. The higher standard deviations for clay soil are due to the various clay mineralogies that can be present, having large effects on water retention characteristics. On the other hand, the variation shown in Table 2 is largely the result of the various geochemical conditions under which the measurements were made. Indeed, State regulators may not have comprehensive data available for a proposed hydrogeologic barrier. As more data become available, the uncertainties may be reduced to primarily measurement error, assuming the investigator knows relevant details about the geochemical environment.

From the distribution of attenuations produced in the Monte Carlo simulations, we simply compute the probability of failure to achieve a target attenuation factor:

$$p(\text{failure}) = \frac{\text{number of Monte Carlo runs that produced } A < 10^{-\varepsilon}}{\text{total number of valid Monte Carlo runs}}$$

The probability of failure for poliovirus to achieve 4-log attenuation was $p = 22/5697$ for the sands. Model users would more likely be interested in tighter soils more likely to be proposed as hydrogeologic barriers. Figure 5 shows the results for poliovirus for silt loams. Probability of failure for the 1-meter thick barrier was $p = 6/2000000$. For this particular set of data, the *Rosetta* clays produced a probability of failure $p = 0/9000000$ for the data shown in Tables 1 and 2.

6 Sensitivity Analysis

Beres and Hawkins (2001) listed the advantages of applying the *Plackett-Burman* (Plackett and Burman, 1946) method of sensitivity analysis. These include the ability to measure two-way interaction effects among parameters, and the freedom to apply any desired domain of plausiblility to input parameters. The reader is referred to Beres and Hawkins (2001) for a detailed description of how to apply the method, and Plackett and Burman (1946) gave the statistical foundation and the optimum cyclic permutations (pattern of parameter variation) of parameter combinations that may be used for a given number of variables.

We considered the 17 input parameters that are used in the model solution. Table 3 lists each parameter and the plausible domains used, based on the means

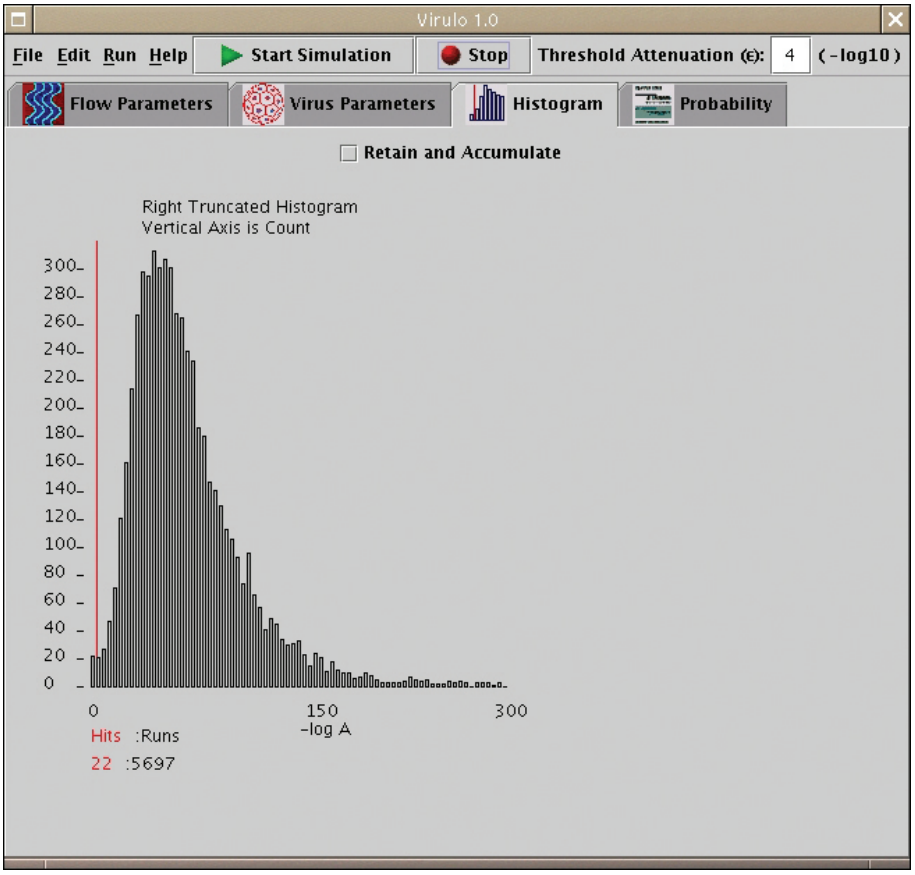

Figure 4: **Frequency histogram of values of $-\log_{10} A$ for poliovirus for Rosetta sands.**

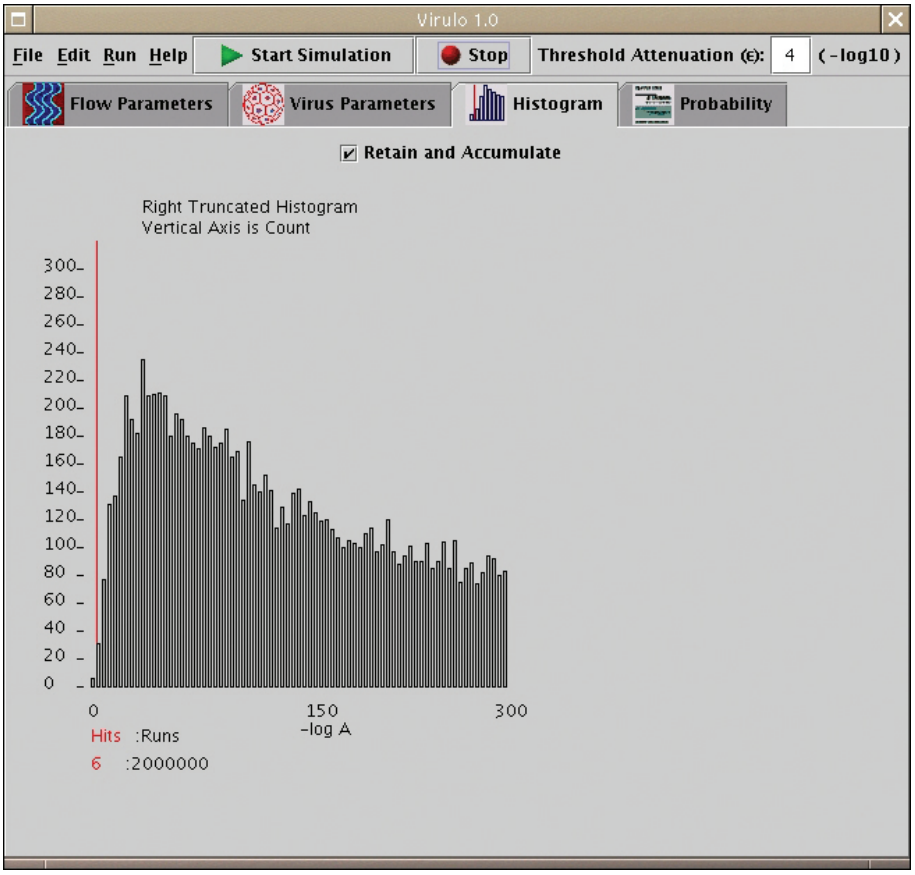

Figure 5: **Frequency histogram of values of $-\log_{10} A$ for poliovirus for Rosetta silt loams.**

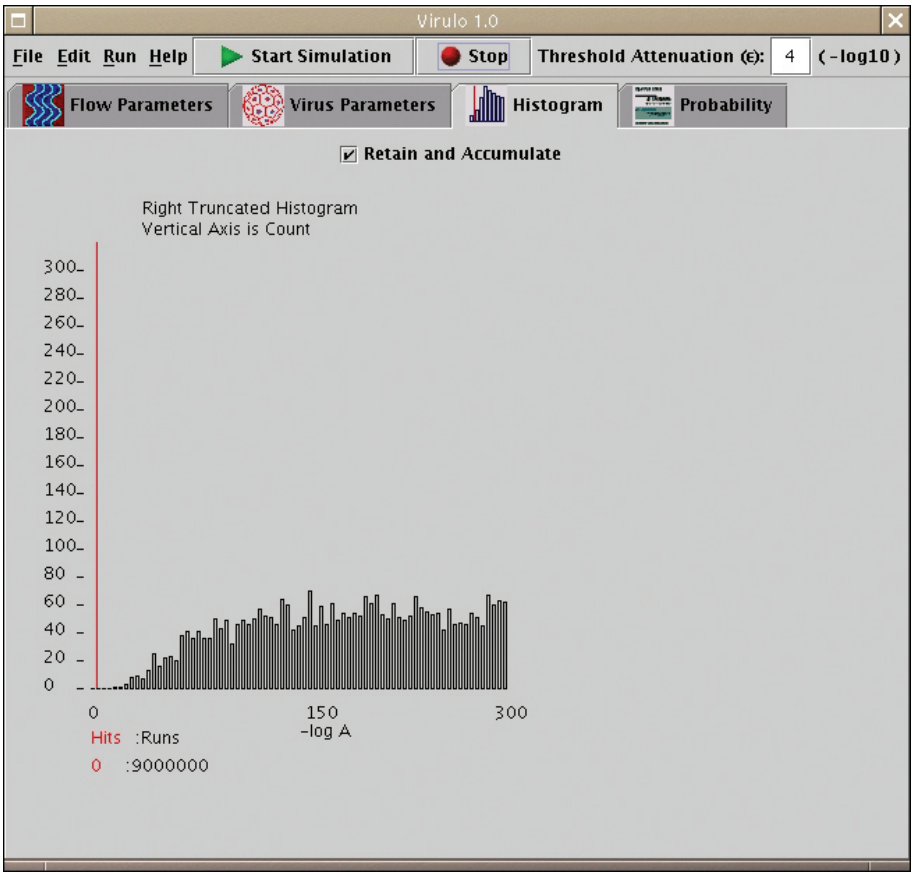

Figure 6: **Frequency histogram of values of $-\log_{10} A$ for poliovirus for Rosetta clays.**

and standard deviations shown in Tables 1 and 2. We used the following cyclic permutation of the parameters, which was derived by Plackett and Burman (1946) for a 20 parameter model:

1	+	+	−	−	+	+	+	−	+	−	+	−	−	−	−	+	+	−
2	−	+	+	−	−	+	+	+	−	+	−	+	−	−	−	−	+	+
3	+	−	+	+	−	−	+	+	+	−	+	−	+	−	−	−	−	+
4	+	+	−	+	+	−	−	+	+	+	−	+	−	+	−	−	−	−
5	−	+	+	−	+	+	−	−	+	+	+	−	+	−	+	−	−	−
6	−	−	+	+	−	+	+	−	−	+	+	+	−	+	−	+	−	−
7	−	−	−	+	+	−	+	+	−	−	+	+	+	−	+	−	+	−
8	−	−	−	−	+	+	−	+	+	−	−	+	+	+	−	+	−	+
9	+	−	−	−	−	+	+	−	+	+	−	−	+	+	+	−	+	−
10	−	+	−	−	−	−	+	+	−	+	+	−	−	+	+	+	−	+
11	+	−	+	−	−	−	−	+	+	−	+	+	−	−	+	+	+	−
12	−	+	−	+	−	−	−	−	+	+	−	+	+	−	−	+	+	+
13	+	−	+	−	+	−	−	−	−	+	+	−	+	+	−	−	+	+
14	+	+	−	+	−	+	−	−	−	−	+	+	−	+	+	−	−	+
15	+	+	+	−	+	−	+	−	−	−	−	+	+	−	+	+	−	+
16	+	+	+	+	−	+	−	+	−	−	−	−	+	+	−	+	+	−
17	−	+	+	+	+	−	+	−	+	−	−	−	−	+	+	−	+	−
18	−	−	+	+	+	+	−	+	−	+	−	−	−	−	+	+	−	+
19	+	−	−	+	+	+	+	−	+	−	+	−	−	−	−	+	+	−
20	−	−	−	−	−	−	−	−	−	−	−	−	−	−	−	−	−	−
21	−	−	+	+	−	−	−	−	+	−	+	−	+	+	+	+	−	+
22	+	−	−	+	+	−	−	−	−	+	−	+	−	+	+	+	−	−
23	−	+	−	−	+	+	−	−	−	−	+	−	+	−	+	+	+	−
24	−	−	+	−	−	+	+	−	−	−	−	+	−	+	−	+	+	+
25	+	−	−	+	−	−	+	+	−	−	−	−	+	−	+	−	+	+
26	+	+	−	−	+	−	−	+	+	−	−	−	−	+	−	+	−	+
27	+	+	+	−	−	+	−	−	+	+	−	−	−	−	+	−	+	−
28	+	+	+	+	−	−	+	−	−	+	+	−	−	−	−	+	−	+
29	−	+	+	+	+	−	−	+	−	−	+	+	−	−	−	−	+	−
30	+	−	+	+	+	+	−	−	+	−	−	+	+	−	−	−	−	+
31	−	+	−	+	+	+	+	−	−	+	−	−	+	+	−	−	−	+
32	+	−	+	−	+	+	+	+	−	−	+	−	−	+	+	−	−	−
33	−	+	−	+	−	+	+	+	+	−	−	+	−	−	+	+	−	−
34	−	−	+	−	+	−	+	+	+	+	−	−	+	−	−	+	+	−
35	−	−	−	+	−	+	−	+	+	+	+	−	−	+	−	−	+	−
36	−	−	−	−	+	−	+	−	+	+	+	+	−	−	+	−	−	+
37	+	−	−	−	−	+	−	+	−	+	+	+	+	−	−	+	−	+
38	+	+	−	−	−	−	+	−	+	−	+	+	+	+	−	−	+	−
39	−	+	+	−	−	−	−	+	−	+	−	+	+	+	+	−	−	−
40	+	+	+	+	+	+	+	+	+	+	+	+	+	+	+	+	+	+

Where the values in Table 3 are greater than zero, the effect is proportional to the probability of failure, and parameters which produce effects less than zero are inversely proportional to the probability of failure.

We may interpret the effect as the expected amount and direction of change in the response (probability of failure to achieve 4-log attenuation) that results from changing the particular parameter by the + and − values given for the plausible domains. It is a *resolution IV* factorial design, on account of the foldover, the lower half of the permutation matrix (Beres and Hawkins, 2001). It is not unexpected that the probability of failure to achieve 4-log attenuation is sensitive to parameters that affect water flow, for the given plausible domains. It should be noted the effects of the correlated hydraulic parameters ($\log_{10}K_s$, θ_s, $\log_{10}n$, θ_r, and $\log_{10}\alpha$) listed in Table 3 are listed only to show the effect of a change in the mean value. A special variance-covariance matrix was calculated for all the parameters of the *UNSODA* database (see Appendix B). This matrix was used in the sensitivity analysis. However, it was not adjusted for the effects in means resulting from the cyclic permutations of the parameter mean values.

For the given plausible domains, logarithm of saturated hydraulic conductivity ($\log_{10}K_s$) was the most important parameter. In light of experimental evidence that preferential flow plays an important role in unsaturated mass transfer, users should do their best to obtain improved estimates of the effective $\log_{10}K_s$ if there is evidence of soils that could produce preferential flow. The second most important parameter was $\kappa^{\diamond}$, the rate of microscopic mass transfer from the suspended phase to the air-water interface, where the viruses are adsorbed, and effectively removed from the system. This result highlights the importance of estimating the

Table 3: **Main Effects on Probability of Failure**

Parameter	Plausible Domain*		Effect
	–	+	
$\log_{10} K_s$	-2.12	0.42	+0.105
$\kappa^{\diamond}$	0.0	0.023	−0.099
L	0.5	20	−0.039
$\log_{10} n$	0.23	0.31	+0.030
r_p	6.233×10^{-5}	1.997×10^{-4}	−0.026
$\log_{10} \lambda$	0.0	1.213	−0.025
$\log_{10} \lambda^*$	0.0	0.912	+0.020
K_d	-3.05×10^{-4}	1.20×10^{-3}	−0.017
θ_r	0.0647	0.0753	+0.015
θ_m	0.15	0.40	+0.012
T	4.32	19.08	+0.007
ρ	975333	1891333	+0.006
$\log_{10} \alpha$	0.12	0.28	+0.005
r_v	1.250×10^{-8}	1.500×10^{-8}	−0.004
κ	0.0	3.14×10^{-3}	+0.002
α_z	8.75×10^{-5}	5.59×10^{-3}	−0.001
θ_s	0.433	0.376	+0.001

* Computed by using the mean of the means $\pm$ the mean of the standard deviations. Computed for θ_m by using mean $\pm$ the standard deviation for the drying curves, "lab" and "field" listed in the UNSODA database.

air-water interfacial area, a difficult endeavor, and an important subject of research for unsaturated-zone contaminant transport.

Two-way interaction effects were also measured. These are listed completely in Appendix C. Most notable among these include $L \times \log_{10}\lambda^*$ (−0.072), which is not surprising due to the increased residence time experienced by the viruses in thicker soil layers, $r_v \times K_d$ (+0.054), and $\log_{10}K_s \times \kappa^{\diamond}$ (−0.095, the parameters which exhibit important (and opposing) main effects.

7 Design of the Computer Model

The Java programming language (Gosling et al., 2000) was used to implement the model. This language allows object- oriented design to be relatively easily implemented. Table 4 lists the classes and interfaces used. Java class documentation will be available on-line and will be described in a forthcoming user's guide for the model. Some of the classes use the *Matrix* class of *JAMA*, a Java matrix package [2].

We consider these classes to be "lightweight," in this context, meaning that they are high-level, easily implemented with other applications, abstracted from the computer hardware and its operating system (i.e., they are *portable*), they have a small footprint, and they require few memory and computational resources.

The model ("Virulo") can be implemented as an applet or application depending on the launcher used (ViruloApplet.java or Virulo.java). The *Swing* graphical components of the Java Foundation Classes were used in the Graphical User Interface (GUI). The model and its source code can be found at

`http://www.epa.gov/ada/`

The classes were written using the *Javadoc* tool [5]. The Javadoc tool uses the philosophy of programming created by Professor Donald Knuth at Stanford University. Knuth advocates that programs should be written to be read not only by machines, but also by humans (Knuth, 1992). He designed a programming language called `WEB`. Programs written in this language are parsed by an engine that generates Pascal source code, as well as source code that can be typeset with Knuth's TEX typesetting program.

The Javadoc commenting system follows a similar philosophy. It is natural to make classes of an object-oriented program easier to read by other programmers so they can be implemented in other programs. This tool allows special comment tags, embedded in the body of the source code, but ignored by the compiler, to be parsed by the Javadoc application. It thus generates formated class documentation that describes the structure and function of the class. Programmers can use it to implement classes without having to resort to reading the Java source code. The Javadoc system generates HTML code in a common style. Much of the HTML document comes from interpreting the Java source code, but the system also allows commenting by the author. Figure 7 shows the Javadoc documentation for the Attenuator class of Virulo.

8 Conclusions

We developed a probabilistic model to predict the effectiveness of a hydrogeologic barrier to pathogenic viruses in the unsaturated zone. It is based on physics, and we can conclude that the following assumptions must be employed:

- Viruses reach the top of the proposed barrier following release in an overlying source, and following their arrival the input concentration decays exponentially. This condition corresponds to an accidental release, such as from an overflowing septic tank, which is subsequently corrected.
- Water flow in the proposed barrier is due to gravity only.
- The virus of interest is approximately spherical in shape.
- The proposed barrier does not contain significant numbers of predatory microorganisms (the model estimate is conservative in this sense).
- The percolating water does not contain significant amounts of surface active agents, such as detergents that could change the hydraulic properties, decay rates, or adsorption.

Table 4: **Classes Used in the Computer Model**

Class	No. of Public Methods	Description
Attenuator	5	Computes the water flux and A.
Compare†	2	Interface for sorting callback (due to Eckel 1998).
DoubleCompare	2	Subclass of *Compare* for sorting callback.
FlowComboPanel extends **JPanel**‡	2	Combo box for selecting soil type
FlowPanel extends **JPanel** implements **Observer**	3	Panel to display flow parameter text boxes.
GasDev	2	Java translation of the popular C program `gasdev.c` (Press et al. 1989).
Gossiper implements **Observer**	1	Observer object (Gamma et al. 1995) that notifies subscribing objects of actions without violating object-orientation by creating unwanted dependencies.
Histogram	4	Polymorphable class for generating histograms.
HistoPlot	2	Uses Histogram to create a **BufferedImage** for display.
HistoPanel extends **JPanel**	1	Panel for displaying histogram image.
HspBasicMath	2	Has useful static methods for oft-used math operations.
HspMonteCarlo	1	Conducts and manages the Monte Carlo Simulations for Virulo.
ImageCanvas	2	Polymorphable image canvas of Geary (1999).
JarLoadable	0	Allows image files to be retrieved on the fly from a Java Archive (jar) file.
Medium implements **Cloneable**	0	Cloneable data structure for soil parameters.
Mvn	1	Generate a realization of a multivariate normal distribution. Behaves like the SAS^{TM} macro `mvn.sas` [3].
Normal implements **Cloneable**	1	Cloneable data structure for a parameter in Virulo.
NormalF	0	Data structure for parameter text fields.
Operandum implements **Cloneable**	1	Cloneable data structure for virus parameters.
OutputPanel extends **JTextPane**	1	Prints clipboardable text output.
Random	2	Polymorphable random deviate generator due to Java Numerical Toolkit [4].
SoilStack	1	Holds necessary parameters for each soil type, selectable with FlowComboPanel.
SortVector	1	Sorts a Java **Vector** object, due to Eckel (1998).
StringAsChars implements **Cloneable**	0	Cloneable data structure for a soil or virus name.
VarCov	1	Stores variance-covariance matrices as computed with *Rosetta* for each soil type.
VectorParser	7	Useful oft-used static methods for use with Java **Vector** objects.
Virulo (or ViruloApplet)	1	Launcher for the application (or applet).
ViruloFrame extends JFrame	1	GUI frame for Virulo.
VirusComboPanel extends **JPanel**	0	The analogy of FlowComboPanel, but for virus parameters.
VirusStack	1	Analogy of SoilStack, but for virus parameters by virus name.

† Names in italics represent Java interfaces.
‡ Names in boldface represent classes that are part of the Java language

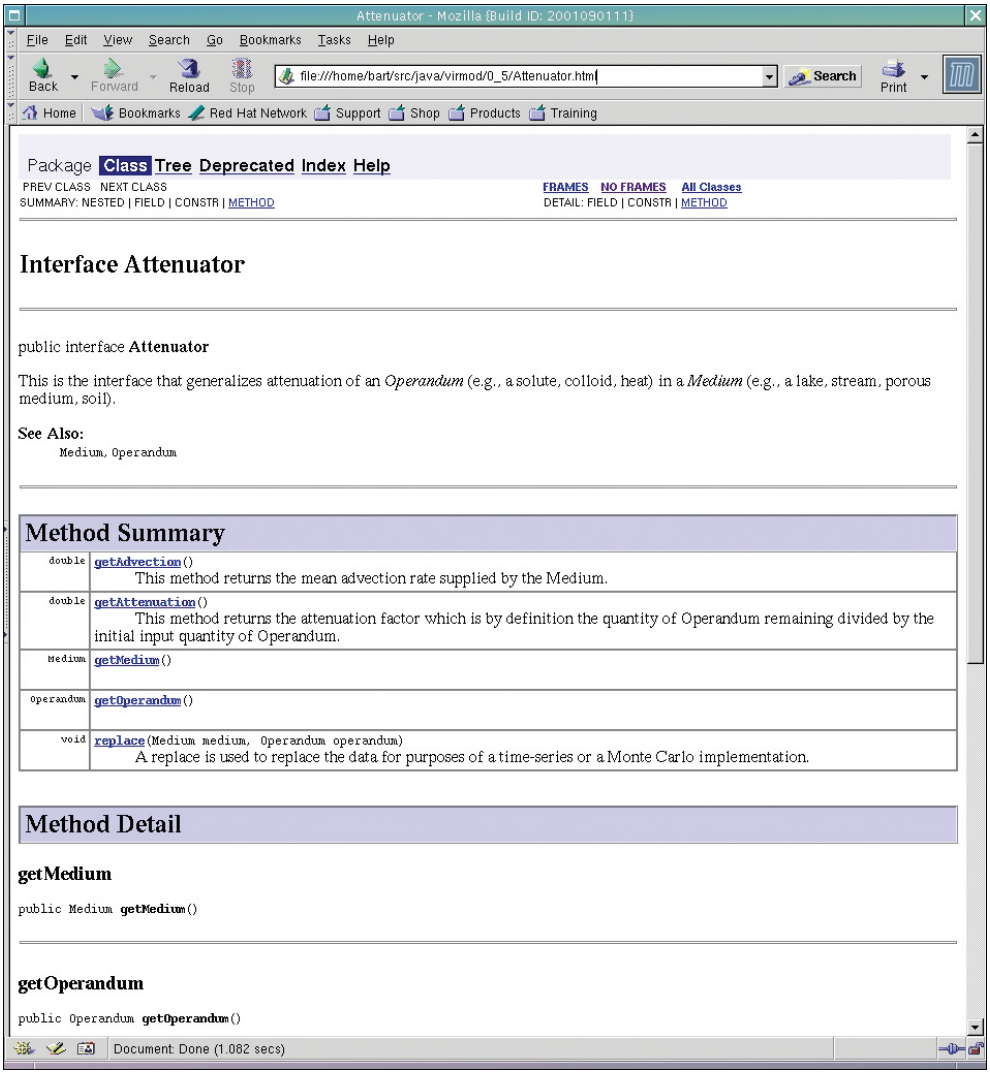

Figure 7: **Javadoc class documentation for Attenuator interface.**

- The proposed barrier matrix consists of one of the 12 USDA soil types.
- Provided distribution functions for saturated hydraulic conductivity do not account for preferential flow, thus it must be assumed preferential flow will not occur in the site of interest.

We found that for a 1-meter thick proposed hydrogeologic barrier with a volumetric water content of 0.3, only soils classified as clays did not fail to produce the 4-log attenuation in the these simulations. User's may have additional information that could change the outcome of the probabilistic model.

This study revealed several areas of much needed research. These include:

- Table 3 lists, in order of magnitude, the parameters that most strongly affect the results of this model. It suggests the parameters which should receive the most research attention through experiments.
- The issue of accurate estimation of the air-water interfacial area is an important one, not only for modeling transport of contaminants subject to hydrophobicity effects, but also for unsaturated-zone virus transport modeling.
- More experimentation is needed with real proteins or the amino-acids that have surfaces that behave like viruses, rather than artificial or inorganic colloids.
- Geochemical effects can produce profound changes in the sorption and survival of the viruses, and more work is needed to identify the causes.
- Although plaque assays are appropriate for testing of natural water for the presence of viruses, the associated uncertainty when large numbers of viruses are used, lead to lack of experimental control at the level of accuracy needed to study viruses in unsaturated soil columns. For these types of studies, more accurate assay methods are needed.
- Correlations need to be developed to predict mass transfer coefficients specifically for viruses which sorb at both the solid-water and the air-water interface. Current correlations are not relevant for viruses.
- Out of about 36 soil column studies in the literature, only those of Jin et al. (2000) and Chu et al. (2001) were done with unsaturated columns. More unsaturated column studies are needed.

Because of the large uncertainty in parameters needed to predict virus transport in the unsaturated zone, probabilistic models that encapsulate and propagate the uncertainty in those parameters in the predictions should be used.

9 List of Symbols and Notation Used

Symbol	Description
α	Water retention curve fitting parameter
α_z	Vertical hydrodynamic dispersivity
β	Coefficient of exponential decay of virus concentration
θ_m	Soil water content
θ_r	Residual soil water content
θ_s	Saturated soil water content
θ_v	Measured water content equivalent to θ_m
κ	Suspended to solid sorbed virus mass transfer coefficient
$\kappa^\diamond$	Suspended to air-sorbed virus mass transfer coefficient
λ	Suspended phase virus inactivation rate
λ^*	Solid-sorbed phase virus inactivation rate
$\lambda^\diamond$	Air-sorbed phase virus inactivation rate
μ	Viscosity of water
ν	General Gaussian random variable
ρ	Soil bulk density
ρ_{pn}	Pearson's correlation coefficient
ρ_w	Density of water
σ	Surface tension of water
$\sigma^2\{\}$	Variance operator
τ	Unsaturated soil water tortuosity
ω	Dummy variable of integration
A	The predicted attenuation factor (C_f/C_{max})
C	Concentration of viruses in suspended phase
C^*	Concentration of viruses in the solid-sorbed phase
$C^\diamond$	Concentration of viruses in the air-sorbed phase
C_{max}	Maximum (initial) concentration of viruses entering top of proposed hydrogeologic barrier
C_f	Concentration of viable suspended viruses exiting the proposed hydrogeologic barrier
$\mathcal{D}$	Molecular virus diffusivity
$\mathcal{D}_e$	Effective molecular virus diffusivity
D_z	Vertical hydrodynamic dispersion coefficient
Da_1	Dahmköhler number for mass transfer, suspended to solid-water interface
Da_3	Dahmköhler number for mass transfer, suspended to air-water interface
$F(t,z)$	Cumulative virus attenuation function
$\tilde{F}(s,z)$	Laplace transform of cumulative virus attenuation function
J_w	Measured flux of percolating water equivalent to q
$K(\theta_m)$	Unsaturated hydraulic conductivity
K_d	Equilibrium distribution coefficient (solid-suspended)
K_s	Saturated hydraulic conductivity
L	Thickness of proposed hydrogeologic barrier
N	Number of observations
S_e	Effective soil water saturation
T	Temperature
$\bar{V}$	Mean percolation velocity
$V_{ox-removed}$	Measured velocity of percolating water
$V_{water-washed}$	Measured velocity of percolating water
$a_T^\diamond$	Air-water interfacial area
a_T	Solid-water interfacial area (soil specific surface area)
$f(t,z)$	Virus attenuation function
g	Acceleration due to gravity
h	Soil capillary pressure head
k	Suspended to solid sorbed virus mass transfer rate
$k^\diamond$	Suspended to air-sorbed virus mass transfer rate
k_1	Mass transfer rate equivalent to k
k_3	Mass transfer rate of equivalent to $k^\diamond$
k_b	Boltzmann's constant
n	Water retention curve fitting parameter
p	Probability
q	Flux of percolating water
$\mathbf{r_p}$	Vector of calculated mean soil particle diameters
r_p	Mean soil particle radius
r_v	Virus radius
s	Laplace domain variable
t	Time
x	General Gaussian random variable
y	General Gaussian random variable
z	Distance downward from top of proposed hydrogeologic barrier

10 References

Anwar, A.H.M.F., Bettahar, M., Matsubayashi, U. 2000. A method for determining air-water interfacial area in variably saturated porous media. *J. Contam. Hydrol.* 43:129-146.

Beres, D.L., Hawkins, D.M. 2001. Plackett-Burman technique for sensitivity analysis of many-parametered models. *Ecol. Modell.* 141:171-183.

Boas, M. 1983. *Mathematical Methods in the Physical Sciences, Second Edition*. John Wiley & Sons, New York. 793 p.

Breidenbach, P., Chattopadhyay, S., Lyon, W.G. Survival and Transport of Viruses in the Subsurface, An Environmental Handbook, U.S. EPA Document in preparation.

Chu. Y., Jin, Y, Flury, M., Yates, M.V. 2001. Mechanisms of virus removal during transport in unsaturated porous media. *Water Resour. Res.* 37(2):253-263.

Eckel, B. 1998. *Thinking in Java* Prentice Hall PTR, Upper Saddle River, New Jersey. 1098 p.

EPA. 2000. National Primary Drinking Water Regulations: Ground Water Rule. *Fed. Regis.* 65(91):30193-30274.

Gamma, E., Helm, R., Johnson, R., Vlissides, J. 1995. *Design Patterns, Elements of Reusable Object-Oriented Software*. Addison-Wesley, Reading, Massachusetts. 395 p.

Geary, D.M. 1999. *Graphic Java^{TM} 2, Mastering the JFC, 3rd Edition, Volume II, Swing*. Sun Microsystems Press, Palo Alto. 1622 p.

Gosling, J., Joy, B., Steele, G., Bracha, G. 2000. *The Java^{TM} Language Specification, Second Edition*. Addison-Wesley, Boston. 505 p.

Hantush, M.M., Mariño, M.A., Islam, M.R. 2000. Models for leaching of pesticides in soils and groundwater. *J. Hydro.* 227:66-83.

Jin, Y., Chu, Y., Yunsheng, L. 2000. Virus removal and transport in saturated and unsaturated sand columns. *J. Contam. Hydrol.* 43:111-128.

Jury, W.A., Gardner, W.R., Gardner, W.H. 1991. *Soil Physics, Fifth Edition*. John Wiley & Sons, Inc. New York. 328 p.

Kaczmarek, M., Hueckel, T., Chawla, V., Imperiali, P. 1997. Transport through a clay barrier with the contaminant concentration dependent permeability. *Transport in Porous Media* 29:159-178.

Keswick, B.H., Gerba, C.P. 1980. Viruses in groundwater. *Environ. Sci. Technol.* 14:1290-1297.

Kim, H., Rao, P.S.C., Annable, M.D. 1997. Determination of effective air-water interfacial area in partially saturated porous media using surfactant adsorption. *Water Resour. Res.* 33(12):2705-2711.

Kitanidis, P.K. 1997. *Introduction to Geostatistics: Applications in Hydrogeology*. Cambridge University Press, Cambridge, U.K. 249 p.

Knuth, D.E. 1992. *Literate Programming, CSLI Lecture Notes Number 27*. Center for the Study of Language and Information, Leland Stanford Junior University. Stanford, California. 368 p.

Lance, J.C., Gerba, C.P. 1984. Effect of ionic composition of suspending solution on virus adsorption by ad soil column. *Environ. Sci. Technol.* 14:1290-1297.

Leij, F.J., Alves W.J., van Genuchten R. 1996. The UNSODA Unsaturated Hydraulic Database, User's Manual Version 1.0. EPA/600/R-96/095.

Lyon, W.G., Faulkner, B.F., Khan, F., Chattopadhyay, S., Cruz, J. 2002. Predicting Attenuation of Viruses in Unsaturated Natural Barriers: 2. User's Guide to Virulo. (in preparation).

Mazzone, H.M. 1998. *CRC Handbook of Viruses*, CRC Press, Boca Raton, FL.

Plackett, R.L., Burman, J.P. 1946. Design of optimum multifactorial experiments. *Biometrika* 33:305-325.

Poletika, N.N., Jury, W.A., Yates, M.V. 1995. Transport of bromide, simazine, and MS-2 coliphage in a lysimeter containing undisturbed, unsaturated soil. *Water Resour. Res.* 31(4):801-810.

Press, W.H., Teukolsky, S.A., Vetterling, W.T., Flannery, B.P. 1992. *Numerical Recipes in C, The Art of Scientific Computing, Second Edition*. Cambridge University Press, Cambridge, U.K. 994 p.

Rose, W., Bruce, W.A. 1949. Evaluation of capillary character in petroleum reservoir rock. *Trans. Am. Inst. Min. Metall. Eng.* 186:127-142.

Schaap, M.G., Leij, F.J., van Genuchten, M.T. 1999. Bootstrap-neural network approach to predict soil hydraulic parameters. (In) M.T. van Genuchten, F.J. Leij, L. Wu (Eds.) *Characterization and Measurement of the Hydraulic Properties of Unsaturated Porous Media, Part 2. Proceedings of the International Workshop*. University of California, Riverside. pp. 1237-1250.

Schaefer, C.E., Arands, R.R., van der Sloot, H.A., Kosson, D.S. 1995. Prediction and experimental validation of liquid-phase diffusion resistance in unsaturated soils. *J. Contam. Hydrol.* 20:145-166.

Schijven, J.F., Hassanizadeh, S.M. 2000. Removal of viruses by soil passage: overview of modeling, processes, and parameters. *Critical Reviews of Environmental Science and Technology* 30(1):49-127.

Sim, Y., Chrysikopoulos, C.V. 2000. Virus transport in unsaturated porous media. *Water Resour. Res.* 36(1):173-179.

Thompson, S.S., Flury, M., Yates, M.V., Jury, W.A. 1998. Role of the air-water-solid interface in bacteriophage sorption experiments. *Appl. Environ. Microbiol.* 64(1):304-309.

Thompson, S.S., Yates, M.V. 1999. Bacteriophage inactivation at the air-water-solid interface in dynamic batch systems. *Appl. Environ. Microbiol.* 65(3):1186-1190.

van Genuchten, M.Th. 1980. A closed-form equation for predicting the hydraulic conductivity of unsaturated soils. *Soil Sci. Soc. Am. J.* 44:892-898

van Genuchten, M.Th., Leij, F.J., Yates, S.R. 1992. The RETC Code for Quantifying the Hydraulic Functions of Unsaturated Soils. EPA/600/S2-91/065. 10 p.

Vilker, V.L, Burge, W.D. 1980. Adsorption mass transfer model for virus transport in soils. *Water Res.* 14:793-790.

Wan, J., Wilson, J.L. 1994. Visualization of the role of the gas-water interface on the fate and transport of colloids in porous media. *J. Appl. Environ. Microbiol.* 60:509-516.

Wilson, E.J., Geankoplis, C.J. 1966. Liquid mass transfer at very low Reynolds numbers in packed beds. *I&EC Fundam.* 5(1):9-14.

Yates, M.V. 1995. Field evaluation of the GWDR's natural disinfection criteria. *J. Am. Water Works Assoc.* 87:76-84.

Yates, M.V. and W.A. Jury. 1995. On the use of virus transport modeling for determining compliance. *J. Environ. Qual.* 24:1051-1055.

Yates, M.V., Ouyang, Y. 1992. VIRTUS, a model of virus transport in unsaturated soils. *Appl. Environ. Microbiol.* 58:1609-1616.

11 Internet References

[1] Mount, H.R. 2000. *Remote Soil Temperature Network*,
`http://www.statlab.iastate.edu/soils/nssc/temperature/rstn1.htm`

[2] *JAMA* : A Java Matrix Package.
`http://math.nist.gov/javanumerics/jama/`

[3] SAS Institute. 2000. *MVN macro: Generating multivariate normal data*, http://ewe3.sas.com/techsup/download/stat/mvn.html

[4] NIST. 1998. *Java Numerical Toolkit*, http://math.nist.gov/jnt/

[5] JAVADOC TOOL HOME PAGE, http://java.sun.com/j2se/javadoc/index.html

Appendix A

Back-Calculation of Mass Transfer Coefficients of Chu et al. (2001)

1. Assume Chu et al. (2001) k_1 is our k and their k_3 is our $k^{\diamond}$, based on Chu et al. Figure 1. Also their J_w is our q, and their θ_v is our θ_m.

2. From Chu et al. Table 1 calculate the velocities as $V_{ox-removed} = J_w/\theta_v = 4.86/0.209 = 23.3cm/hr$ and $V_{water-washed} = 1.14/0.24 = 4.75\ cm/hr = 0.0475\ m/hr$

3. Experiment 1 obtained $Da_3 = 2.92$ at $V_{ox-removed} = 23.3$ cm/hr, thus $k^{\diamond}_{MS-2} = V_{ox-removed} Da_3/L = (23.3cm/hr)(2.92)/(10cm) = 6.80hr^{-1}$
Experiment 2 obtained $Da_1 = 12.1$ at $V_{water-washed} = 4.74$ cm/hr, thus $k_{MS-2} = 5.74hr^{-1}$

4. Let $'$ refer to values obtained from the sand centroid of the soil triangle. Now

   $a_T = \frac{3(1-\theta_{s'})}{r_{p'}} = \frac{3(1-0.37)}{0.044cm} = 42.95\ cm^{-1} = 4295\ m^{-1}$
   $\Rightarrow \kappa_{MS-2} = 5.75/42.95 = 0.134$ cm/hr=0.00134 m/hr

5. $a^{\diamond}_T = \frac{\rho_w g \theta_m}{\alpha\sigma}\left[\left(\frac{\theta_s-\theta_r}{\theta_m-\theta_r}\right)^{\frac{1}{1-1/n}} - 1\right]^{1/n}$
   if $\theta_m = \theta_{v(Chu)}$ and other values taken from sand centroid, then
   $a^{\diamond}_T = 7.333\ cm^{-1} = 733.3\ m^{-1}$
   and
   $\kappa^{\diamond}_{MS-2} = 6.80/7.333 = 0.927$ cm/hr=0.00927 m/hr

6. To compute the propagation of error let $\sigma^2\{\}$ be the variance operator. Then according to Boas (1983) p. 734, consider a function ν of 2 normally distributed variables, x and y. We use overlines to denote the mean. If they are uncorrelated, then

   $$\text{Var}\,[\overline{\nu}] = \left(\frac{\partial\nu}{\partial x}\right)^2 \sigma^2\{\overline{x}\} + \left(\frac{\partial\nu}{\partial y}\right)^2 \sigma^2\{\overline{y}\}\Bigg|_{x=\overline{x},\ y=\overline{y}}$$

   From the *UNSODA* database, we estimated mean particle radii, for each soil classified as sand, from sieve data as follows:

a	**b**	**c**
sieve size	particle fraction	weighted component
a_1	b_1	$((a_1 - a_0)/2 + a_0) \times b_1$
a_2	b_2	$((a_2 - a_1)/2 + a_1) \times b_2$
a_3	b_3	$((a_3 - a_2)/2 + a_2) \times b_3$
$\vdots$	$\vdots$	$\vdots$
a_n	b_n	$((a_n - a_{n-1})/2 + a_{n-1}) \times b_n$
		$\mathbf{r_p} = \frac{1}{2}\sum b_i$

With this we obtained an overall mean, $\overline{\mathbf{r_p}} = 1.73 \times 10^{-4}\ m$, and a standard deviation $\sigma\{\mathbf{r_p}\} = 9.1 \times 10^{-5}$. These are the values listed in Table 1.

We then computed Pearson's correlation coefficient (ρ_{pn}) between these computed r_p values and the values of θ_s for the *UNSODA* database which were fitted with the least squares computer program *RETC*. We obtained the following:

$\rho_{pn} = -0.137$
number of observations: 93
Under $H_0 : \rho_{pn} = 0$,
we obtained $p = 0.191$, thus we cannot reject the null hypothesis, and conclude θ_s and r_p are uncorrelated for soils classified as sand.

Thus we may proceed using the propagation of error formula listed above:

$$\text{Var}[\overline{a_T}] = \left(\frac{\partial a_T}{\partial \theta_{s'}}\right)^2 \sigma^2\{\overline{\theta}_{s'}\} + \left(\frac{\partial a_T}{\partial r_{p'}}\right)^2 \sigma^2\{\overline{r}_{p'}\} \Bigg|_{\theta_{s'}=\overline{\theta}_{s'},\ r_{p'}=\overline{r}_{p'}}$$

Noting that

$\frac{\partial a_T}{\partial \theta_{s'}} = -\frac{3}{r_{p'}}$
$\frac{\partial a_T}{\partial r_{p'}} = -\frac{3(1-\theta_{s'})}{r_{p'}^2}$
And evaluating at the means, we obtain:
$\text{Var}[a_T] = 3.33 \times 10^7$

In a likewise manner, we obtain
$\text{Var}[\kappa] = 3.235 \times 10^{-6}$

Due to the lack of data on $\kappa^\diamond$ we assume the only significant contributions to the error in $\kappa^\diamond$ are the lack of fit error in the Dahmköhler number as computed by Chu et al. plus the error in $a_T^\diamond$ is of similar magnitude as that of a_T. We also note $\sigma^2\{lack\ of\ fit\} \ll \sigma^2\{a_T\}$, then

$\text{Var}[\kappa^\diamond] \approx \text{Var}[\kappa]$

Appendix B.

Variance-Covariance Matrices of Correlated Hydraulic Parameters

		θ_r	θ_s	$\log_{10}\alpha$	$\log_{10}n$	$\log_{10}K_s$
sand						
	θ_r	+0.00001	+0.00003	-0.00009	+0.00012	+0.00042
	θ_s	+0.00003	+0.00103	+0.00021	-0.00038	+0.00191
	$\log_{10}\alpha$	-0.00009	+0.00021	+0.00113	-0.00185	-0.00446
	$\log_{10}n$	+0.00012	-0.00038	-0.00185	+0.00593	+0.01506
	$\log_{10}K_s$	+0.00042	+0.00191	-0.00446	+0.01506	+0.04731
silt loam						
	θ_r	+0.00016	+0.00049	-0.00015	+0.00000	-0.00050
	θ_s	+0.00049	+0.00251	-0.00146	+0.00030	+0.01017
	$\log_{10}\alpha$	-0.00015	-0.00146	+0.00560	-0.00114	-0.01506
	$\log_{10}n$	+0.00000	+0.00030	-0.00114	+0.00026	+0.00425
	$\log_{10}K_s$	-0.00050	+0.01017	-0.01506	+0.00425	+0.14744
clay						
	θ_r	+0.00011	+0.00090	+0.00110	-0.00006	+0.00469
	θ_s	+0.00090	+0.00727	+0.00871	-0.00038	+0.03863
	$\log_{10}\alpha$	+0.00110	+0.00871	+0.01676	-0.00152	+0.04797
	$\log_{10}n$	-0.00006	-0.00038	-0.00152	+0.00023	-0.00179
	$\log_{10}K_s$	+0.00469	+0.03863	+0.04797	-0.00179	+0.22576
everything*						
	θ_r	+0.00034	+0.00103	-0.00262	-0.00099	-0.00430
	θ_s	+0.00103	+0.00469	-0.00718	-0.00293	+0.00016
	$\log_{10}\alpha$	-0.00262	-0.00718	+0.09467	+0.01776	+0.12027
	$\log_{10}n$	-0.00099	-0.00293	+0.01776	+0.02035	+0.08733
	$\log_{10}K_s$	-0.00430	+0.00016	+0.12027	+0.08733	+0.52026

* Includes all 12 USDA soil categories.

Appendix C

Complete List of Two-Way Interaction Effects Among *Virulo* Parameters.

	θ_r	θ_m	θ_s	$\log_{10} K_s$	$\log_{10}\alpha$	$\log_{10} n$	ρ	r_p	$\log_{10}\alpha_z$	T	L	$\log_{10}\lambda$	$\log_{10}\lambda^*$	κ	$\kappa^\diamond$	r_v
θ_r	·	·	·	·	·	·	·	·	·	·	·	·	·	·	·	·
θ_m	−0.033	·	·	·	·	·	·	·	·	·	·	·	·	·	·	·
θ_s	+0.070	−0.007	·	·	·	·	·	·	·	·	·	·	·	·	·	·
$\log_{10} K_s$	+0.017	+0.013	+0.002	·	·	·	·	·	·	·	·	·	·	·	·	·
$\log_{10}\alpha$	−0.019	−0.024	−0.032	+0.005	·	·	·	·	·	·	·	·	·	·	·	·
$\log_{10} n$	+0.008	−0.006	−0.016	+0.033	+0.046	·	·	·	·	·	·	·	·	·	·	·
ρ	−0.005	+0.003	−0.032	+0.008	+0.024	−0.014	·	·	·	·	·	·	·	·	·	·
r_p	+0.004	−0.014	+0.033	−0.027	−0.049	−0.021	−0.027	·	·	·	·	·	·	·	·	·
$\log_{10}\alpha_z$	+0.022	−0.071	−0.006	−0.003	−0.001	−0.005	−0.023	−0.009	·	·	·	·	·	·	·	·
T	−0.049	+0.033	−0.030	+0.009	−0.028	−0.034	+0.040	−0.019	−0.013	·	·	·	·	·	·	·
L	+0.002	−0.025	−0.015	−0.035	−0.002	−0.030	+0.024	+0.010	+0.002	−0.010	·	·	·	·	·	·
$\log_{10}\lambda$	+0.000	−0.041	+0.026	−0.021	+0.000	−0.049	−0.034	+0.012	+0.055	−0.014	−0.016	·	·	·	·	·
$\log_{10}\lambda^*$	−0.022	+0.038	−0.008	+0.021	+0.025	+0.041	−0.033	−0.023	−0.026	−0.013	−0.072	+0.007	·	·	·	·
κ	−0.026	+0.021	−0.014	+0.004	−0.014	+0.023	+0.018	+0.051	−0.043	+0.027	−0.033	−0.032	+0.023	·	·	·
$\kappa^\diamond$	−0.018	−0.013	−0.002	−0.095	−0.004	−0.029	−0.006	+0.030	+0.000	−0.007	+0.032	+0.023	−0.024	−0.006	·	·
r_v	+0.027	+0.025	+0.001	−0.005	−0.039	−0.023	−0.005	+0.007	−0.013	−0.025	+0.034	−0.022	−0.013	−0.030	+0.007	·
K_d	−0.001	+0.006	−0.017	−0.014	−0.033	+0.004	−0.047	+0.034	+0.018	−0.034	+0.029	−0.015	−0.013	−0.009	+0.014	+0.054

United States
Environmental Protection
Agency

National Risk Management
Research Laboratory
Cincinnati, OH 45268

Official Business
Penalty for Private Use
$300

EPA/600/R-02/051a
August 2002

Please make all necessary changes on the below label, detach or copy, and return to the address in the upper left-hand corner.

If you do not wish to receive these reports CHECK HERE ☐; detach, or copy this cover, and return to the address in the upper left-hand corner.

PRESORTED STANDARD
POSTAGE & FEES PAID
EPA
PERMIT No. G-35